Role of defective icosahedra in undercooled copper

Massimo Celino and Vittorio Rosato*
ENEA, Ente per le Nuove Tecnologie, Energia e Ambiente, Centro Ricerche Casaccia, Casella Postale 2400, 00100 Roma, Italy

Andrea Di Cicco†
IMPMC, Université Paris 6 et 7, CNRS, IPGP, 140 rue de Lourmel, 75015 Paris, France

Angela Trapananti
European Synchrotron Radiation Facility, 6 Rue Jules Horowitz, Boîte Postale 220, F-38043 Grenoble Cedex, France

Carlo Massobrio
Institut de Physique et de Chimie des Matériaux de Strasbourg, 23 rue du Loess, Boîte Postale 43, F-67034 Strasbourg, Cedex 2, France
(Received 23 February 2007; published 31 May 2007)

We elucidate the role played by defective icosahedra on the stability of undercooled copper by using molecular-dynamics simulations. Our approach is substantiated by the level of agreement with experiments on a variety of structural properties. We show that not only perfect but also defective icosahedra, embedded in a disordered matrix, lower the local cohesive energy. This has the effect of stabilizing the liquid structure against crystallization. Our work rationalizes experimental findings by identifying the nature of those icosahedral subunits that contribute to the stability of the undercooled liquid.

DOI: 10.1103/PhysRevB.75.174210 PACS number(s): 61.20.Ja, 61.25.Mv, 64.70.Dv

The remarkable stability of undercooled metals against crystallization has fostered intense research efforts since the pioneering studies of Turnbull.[1] The physical nature of this phenomenon has proved to be largely elusive, calling for interpretations based on atomic-scale arguments. In the search of the microscopic origins underlying this stability, the role played by the icosahedral short-range order (ISRO) has been frequently invoked.[2,3] A conclusive assessment of the ISRO has proved to be challenging for both experiments and theory.[4–8] In this paper, we provide a quantitative description of ISRO in a prototypical undercooled metal (copper) and a rationale for its stability against crystallization. Our calculations settle the controversy on the number of icosahedral structural units by substantially enriching the indications of previous phenomenological analysis.[5,8] We use extensive molecular-dynamics (MD) simulations, based on an *n*-body interatomic potential derived by a second-moment approximation of the tight-binding scheme for *d*-band transition metals.[9] The topology of the local structure is characterized in terms of a common-neighbor analysis and total-energy calculations. This allows us to identify (a) the nature of ISRO in terms of defective icosahedral clusters, (b) the role played by the ISRO to stabilize the undercooled liquid, and (c) the driving force for this stabilization in terms of atomic energy contributions.

MD simulations are widely used to characterize both the glassy and the liquid phase of metals[10–14] in terms of ISRO. The classical version of MD, based on empirical potentials, has proved to be highly reliable in describing the structural features of metals in very diverse thermodynamic conditions, including undercooled metals.[9,10,15,16] A recent paper on liquid nickel has demonstrated that effective-pair potentials can lead to a close agreement with first-principles molecular-dynamics simulations.[17] In the specific case of liquid copper, no intrinsic loss of accuracy is encountered since the performances of potentials and first-principles schemes have been found comparable.[12] In the present work, we rely on classical interatomic potentials to afford system sizes and temporal trajectories not currently achievable within the first-principles MD approach.[11,12,18] We are able to collect a statistically significant number of configurations involving atoms participating to ISRO.

Three systems of 4000 atoms, initially arranged in fcc crystal structures in cubic cells of linear sizes $L=38.47$ Å, $L=38.14$ Å, and $L=30.01$ Å, were subsequently melted to reproduce liquid and undercooled copper at zero pressure and at the temperatures $T=1623$ K, $T=1400$ K, and $T=1313$ K. In each simulation, the average distance covered by the atoms in the liquid (more than 40 Å) ensures that the final configurations retain no memory of the initial geometries. The quench from the equilibrated liquid states ($T=2000$ K) down to the three temperatures has been performed in the *NPT* ensemble using the Parrinello-Rahman and Nosé[19] scheme. For the liquid (at $T=1623$ K and $T=1400$ K) and the undercooled ($T=1313$ K) liquid copper structures, the densities agree with the experimental values[20] within 5%. After 100 ps of annealing at the final temperature, statistical averages and relevant data for structural analysis have been calculated over time trajectories of 200 ps. Hereafter, we shall concentrate on the results at $T=1623$ K and $T=1313$ K.

Recent experimental studies have confirmed the presence of ISRO in simply undercooled metals, with no consensus on the fraction of atoms involved and on the nature of the substructural icosahedral units.[4–8] By following an alternative strategy, the reverse Monte Carlo (RMC) method, combined with accurate x-ray-absorption spectroscopy (XAS), led to an estimate for the fraction of nearly icosahedral clusters.[5,8] These results substantiated the presence of defective icosahedra units. Given these pieces of evidence, unambiguous theoretical tools are expected to bring new, compelling information.

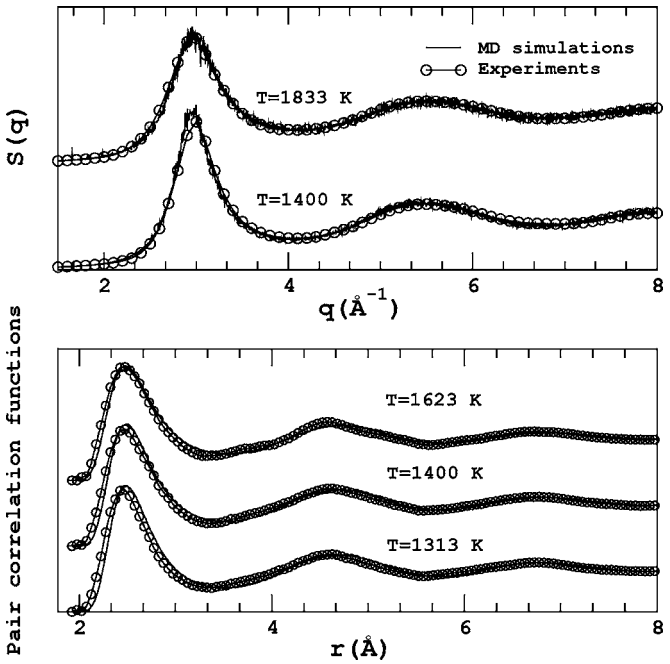

FIG. 1. Upper panel: comparison between calculated neutron structure factor $S(q)$ and experimental nuclear diffraction results (Ref. 21). Lower panel: comparison between pair correlation functions calculated using MD and RMC-XAS results (open circles, see Ref. 5).

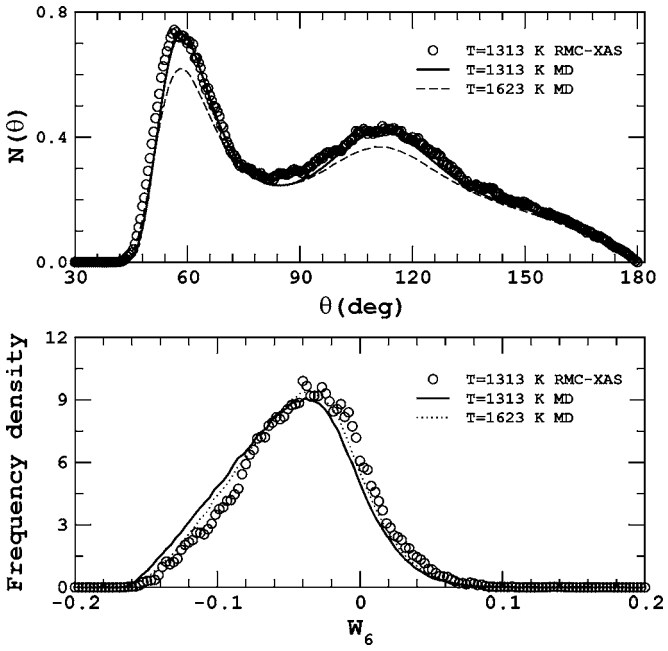

FIG. 2. Upper panel: comparison between calculated and RMC-XAS (open circles, see Ref. 5) bond-angle distributions $N(\theta)$. Lower panel: frequency density of the $\hat{W}_6$ cubic invariant obtained by MD in this work compared with the results of previous RMC data analysis (Ref. 5).

The calculated static structure factor reproduces the neutron-scattering measurements[21] over the entire range of wave vectors (Fig. 1, upper panel). This proves that all interatomic distances are well described by our model at the indicated temperatures in the liquid regime. With respect to the behavior in the undercooled liquid regime, convincing evidence comes from Fig. 1 (lower panel), where the calculated radial correlation functions $g(r)$ at $T=1313$ K are compared with the $g(r)$ obtained by RMC modeling of XAS and diffraction data.[5] The calculated self-diffusion coefficient D ($D=3.90\times10^{-5}$ cm^2/s at $T=1400$ K) is in very good agreement with the experimental value of $D=3.97\times10^{-5}$ cm^2/s at the melting temperature $T=1356$ K.[22] The same holds for the bond-angle distribution $N(\theta)$, for which the comparison with RMC data is shown in Fig. 2 (upper panel). At each temperature, $N(\theta)$ shows two main peaks: one at 60° (equilateral triangles) and another broad maximum around 110°. By lowering the temperature, the height of the peak at 60° increases, giving indications about the onset of icosahedral order in the atomic structure. In Ref. 5, the occurrence of ISRO was monitored using a cubic invariant of spherical harmonics ($\hat{W}_6$).[23] This quantity is particularly sensitive to the presence of icosahedral subunits. In Fig. 2 (lower panel), we report the comparison between the present MD results and the RMC data analysis for $\hat{W}_6$. The good level of agreement demonstrates that the essential features of short-range ordering are well reproduced by our calculations. Some differences between RMC and MD calculation data remain noteworthy in Fig. 2 (lower panel). The origin of these differences has to be ascribed, at least partially, to the nonunique character of the RMC fit to the XAS data.

A deeper insight into the presence and the nature of icosahedral units in the atomic configurations can be obtained from the common-neighbor analysis introduced in Refs. 24 and 25. Each pair of nearest-neighbor atoms is classified by using a set of three indices jkl: j is the number of nearest neighbors common to both atoms, k is the number of bonds between the common neighbors, and l is the number of bonds in the longest continuous chain formed by the k bonds between common neighbors. For example, 421 and 422 pairs are peculiar of fcc and hcp orders. The icosahedral order, in turn, is characterized by bonded pairs of type 555. In a perfect icosahedron, deformations causing the presence of a broken bond between a pair of outer atoms transform 2 of the 555 pairs into 544 and 433 pairs.

To highlight the impact of defective icosahedra, we labeled each atom by the number N_{555} of its 555-type nearest neighbors. Accordingly, for an atom at the center of an icosahedron, N_{555} is equal to 12 (hereafter, termed perfect icosahedra, distortions notwithstanding). In Table I, we report the percentage of atoms in the supercooled liquid with $N_{555} \in [0,12]$ and, for the sake of comparison, the corresponding values in the liquid case ($T=1623$ K). Atoms involved in 421 pairs, reminiscent of crystalline fcc structures, are also found in the undercooled system, as well as those arranged in a bcc fashion (also given in Table I). Perfect icosahedra are present both in the liquid and undercooled systems: in the latter, only 0.26% of the atoms has $N_{555}=12$, whereas in the former, there is a marked decrease (0.11%). One notes that the number of units with $N_{555}=11$ and $N_{555}=10$ is very small. Interestingly, the inclusion of atoms for which $N_{555}\geqslant 6$ in the counting of those responsible of defective icosahedra yields 9.15% for the undercooled liquid. Much smaller values are

TABLE I. First column: percentages of atoms with a selected number of nearest neighbors N_{xxx} and a given symmetry xxx. Second and third columns: the icosahedral (ICO) symmetry is identified by counting N_{555}. Fourth and fifth columns: fcc and bcc symmetries are identified by counting N_{421} and $N_{444}+N_{666}$ nearest neighbors, respectively.

N_{xxx}	ICO $T=1623$ K	ICO $T=1313$ K	fcc $T=1313$ K	bcc $T=1313$ K
0	30.32	20.90	43.62	33.58
1	24.67	22.27	24.70	23.94
2	17.57	18.40	16.94	17.25
3	11.33	13.63	9.08	11.34
4	7.19	9.77	3.39	6.59
5	3.92	5.85	1.54	3.55
6	2.53	4.26	0.53	1.97
7	1.10	2.03	0.12	1.04
8	0.93	1.86	0.06	0.39
9	0.14	0.29	0.01	0.14
10	0.20	0.48	<0.01	0.11
11	<0.01	<0.01	<0.01	0.04
12	0.11	0.26	<0.01	0.02

obtained for fcc and bcc seeds. This agrees with recent experimental results reporting about 10% of atoms involved in the icosahedral order.[5] To validate this comparison, we introduce in what follows an argument based on the potential energy which allows us to identify which atoms do contribute to defective icosahedral order and why. This allows us to go beyond recent achievements obtained through similar techniques where no quantitative correlations between topology and energetics were established.[26]

In Fig. 3, we have reported relative atomic potential energies E_{arel} as a function of N_{555}, the number of 555-type neighbors for each atom in the undercooled liquid. These quantities have been calculated with respect to the average potential energy, i.e., the cohesive energy of the system. E_{arel} is given by $(E_{at}-E_{co})/E_{co}$, where E_{at} is the mean potential energy of atoms with a given number of 555-type neighbors and E_{co} is the average cohesive energy of the system. The two sets of data refer to the potential energies at $T=1313$ K and to the potential energies of the quenched system resulting from rapid cooling to $T=0$ K. The second set of configurations (dashed line) has been created to extract the contributions due to the potential energy, devoid of any entropic effect at finite temperatures. Error bars are smaller than 0.1% throughout. The trend of E_{arel} reveals that the stabilization due to the energy is a decreasing function of N_{555} for $N_{555}<6$. For $N_{555}\geqslant 6$, the nonmonotonic behavior features values smaller (or not significantly higher) than the one pertaining to the perfect icosahedra ($N_{555}=12$). Therefore, atoms with $N_{555}\geqslant 6$ have a more favorable environment in terms of potential energy. This proves that defective icosahedra are at very origin of the structural stability of the undercooled liquid. We reiterate that by using our rationale for the count of the relevant units, we obtain a fraction of icosahedral defective configurations (9.15%) very close to that

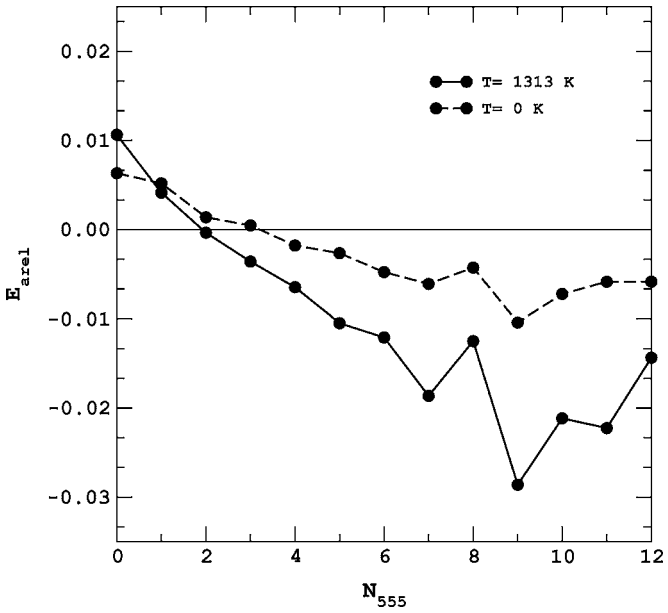

FIG. 3. Full line: relative atomic potential energy E_{arel} as a function of the number of 555-type nearest neighbor N_{555} for each atom. The temperature is $T=1313$ K. Dashed line: the same quantity for a sample quenched at $T=0$ K. The zero value corresponds to the cohesive energies of the systems. By calling the atomic potential energy E_{at} and the cohesive energy of the system E_{co}, E_{arel} is given by $(E_{at}-E_{co})/E_{co}$. Values of E_{co} are -3.21 eV at $T=1313$ K and -3.39 eV after quench at $T=0$ K.

obtained in Ref. 5 by using the $(\hat{W}_6)$ invariant.

The remarkable similarity between the two trends shown in Fig. 3 highlights the predominance of energy effects over the entropic ones. The role of entropy and temperature amounts to increasing the range of the energy variation, with no effect on the identification of the relevant defective icosahedra. Also, shell closing geometric effects are at the origin of maxima and minima observable for $N_{555}\geqslant 6$ when energy and entropy are taken into account. However, these features largely disappear when one focuses on the pure contribution of the potential energy (dashed line).

The question arises on the comparative behavior of the atomic potential energy as a function of other sets of configurations, such as N_{421}, N_{422}, and $N_{555}+N_{666}$. In Fig. 4, we show that N_{555} is the only configuration featuring two distinct trends, i.e., a stabilization regime followed by nonmonotonic variations for larger values. In addition, the atomic energy is systematically lower for N_{555} (the only exception being $N_{555}+N_{666}=8$). This confirms the predominant role played by N_{555} in stabilizing defective icosahedral order.

Our analysis is supported by a visual inspection of Fig. 5 where we focus on the subset of atoms for which $N_{555}\geqslant 6$. Such subset is spread all over the simulation cell exhibiting chains and clusters that delimit regions of high stability. Perfect icosahedral clusters of higher order, such as dodecahedra, supposed to be present[4] are not detected. The total number of atoms involved in the icosahedral order is obtained by computing the number of atoms that are at the center of icosahedral units (i.e., atoms with $N_{555}\geqslant 6$) plus the first shell of their nearest neighbors with $N_{555}<6$. Thus, we esti-

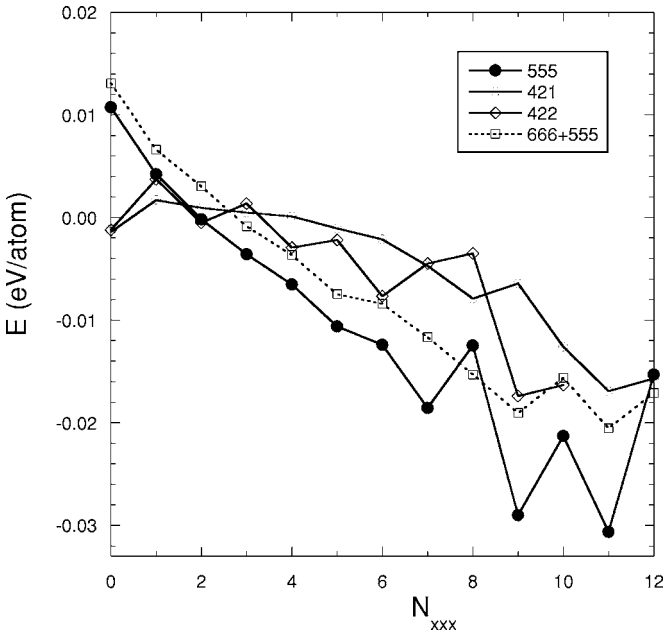

FIG. 4. Relative atomic potential energy E_{arel} as a function of the number of N_{xxx} for several combinations of *xxx* at the temperature $T=1313$ K.

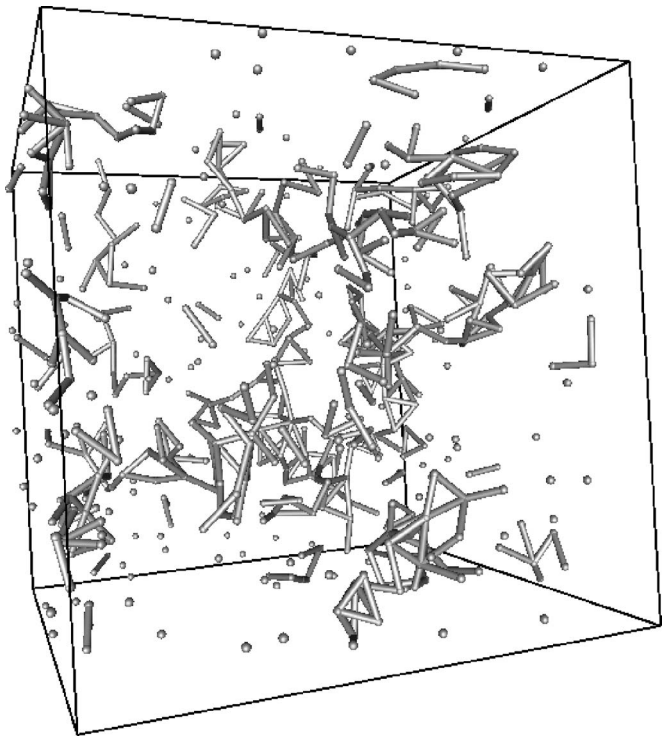

FIG. 5. Snapshot of the undercooled liquid where atoms with $N_{555}<6$ are deleted (see text).

mate that the spatial extension of icosahedral short-range order involves more than 70% of the whole undercooled system. The picture emerging reveals that the undercooled liquid is composed by complex and large structures characterized by icosahedral ordered regions of high stability. These regions are embedded in a disordered atomic structure where fragments reminiscent of the crystalline phase can also be found.

Table I shows that a large fraction of icosahedral atoms forms below the melting point. Their higher stability with respect to fcc (or bcc) atoms may prevent the formation of large units reflecting fcc (or bcc) arrangements, ultimately leading to crystallization. Clustering of icosahedral regions shown in Fig. 5 leads to a growth of the icosahedral seeds which will systematically increase their size from a few tens to a few hundreds atoms.[27] The growth mechanism would also be favored by an enhancement of the fraction of the icosahedral atoms in the sample. However, it is commonly accepted that the relative stability of perfect and isolated icosahedral clusters with respect to fcc-based ones is a decreasing function of their size.[28] Therefore, as soon as the number of atoms forming the icosahedral cluster overcomes a critical threshold, fcc-based clusters become energetically favored.

A careful analysis of atomic configurations generated by MD simulations has proved able to rationalize experimental data on undercooled liquid copper. Within the limits of a theoretical description based on effective potential, this has allowed us to elucidate the role played by defective icosahedra through a precise identification of the geometric environment of each atom. This work shows that the energy associated with defective icosahedra, embedded in the disordered system, lowers the overall energy and stabilizes the undercooled metal preventing crystallization.

*Also at Ylichron s.r.l., C.R. Casaccia, CP 2400, 00100 Roma, Italy.
†Permanent address: CNISM, CNR-INFM CRS SOFT, Dipartimento di Fisica, Università di Camerino, Via Madonna delle Carceri 62032, Camerino (MC), Italy.

[1] D. Turnbull, J. Chem. Phys. **20**, 411 (1952).
[2] F. C. Frank, Proc. R. Soc. London, Ser. A **215**, 43 (1952).
[3] F. Spaepen, Nature (London) **408**, 781 (2000).
[4] T. Schenk, D. Holland-Moritz, V. Simonet, R. Bellissent, and D. M. Herlach, Phys. Rev. Lett. **89**, 075507 (2002).
[5] A. Di Cicco, A. Trapananti, S. Faggioni, and A. Filipponi, Phys. Rev. Lett. **91**, 135505 (2003).
[6] K. F. Kelton, G. W. Lee, A. K. Gangopadhyay, R. W. Hyers, T. J. Rathz, J. R. Rogers, M. B. Robinson, and D. S. Robinson, Phys. Rev. Lett. **90**, 195504 (2003).
[7] G. W. Lee, A. K. Gangopadhyay, K. F. Kelton, R. W. Hyers, T. J. Rathz, J. R. Rogers, and D. S. Robinson, Phys. Rev. Lett. **93**, 037802 (2004).
[8] W. K. Luo, H. W. Sheng, F. M. Alamgir, J. M. Bai, J. H. He, and E. Ma, Phys. Rev. Lett. **92**, 145502 (2004).
[9] F. Cleri and V. Rosato, Phys. Rev. B **48**, 22 (1993).
[10] L. Hui and F. Pederiva, Chem. Phys. **304**, 261 (2004).

[11] N. Jakse and A. Pasturel, Phys. Rev. Lett. **91**, 195501 (2003).
[12] A. Pasquarello, K. Laasonen, R. Car, C. Lee, and D. Vanderbilt, Phys. Rev. Lett. **69**, 1982 (1992).
[13] H. Pang, Z. H. Jin, and K. Lu, Phys. Rev. B **67**, 094113 (2003).
[14] C. Kuiying, L. Hongbo, L. Xiaoping, H. Qiyong, and H. Zhuangqi, J. Phys.: Condens. Matter **7**, 2379 (1995).
[15] J. C. González, V. Rodrigues, J. Bettini, L. G. C. Rego, A. R. Rocha, P. Z. Coura, S. O. Dantas, F. Sato, D. S. Galvao, and D. Ugarte, Phys. Rev. Lett. **93**, 126103 (2004); F. Sato, A. S. Moreira, J. Bettini, P. Z. Coura, S. O. Dantas, D. Ugarte, and D. S. Galvao, Phys. Rev. B **74**, 193401 (2006).
[16] P. Geysermans, M. Mareschal, and V. Pontikis, Mol. Phys. **95**, 465 (1998).
[17] N. Jakse and A. Pasturel, J. Chem. Phys. **123**, 244512 (2005).
[18] P. Ganesh and M. Widom, Phys. Rev. B **74**, 134205 (2006). In this paper, first-principles molecular-dynamics simulation of liquid and undercooled liquid copper is performed on a periodic system of 100 copper atoms.
[19] M. Parrinello and A. Rahman, J. Appl. Phys. **52**, 7182 (1981); S. Nosé, Mol. Phys. **52**, 255 (1984); J. Chem. Phys. **81**, 511 (1984).
[20] Y. Waseda, *The Structure of Non-Crystalline Materials* (McGraw-Hill, New York, 1980).
[21] O. J. Eder, E. Erdpresser, B. Kunsch, H. Stiller, and M. Suda, J. Phys. F: Met. Phys. **10**, 183 (1980).
[22] J. Mei and J. W. Davenport, Phys. Rev. B **42**, 9682 (1990).
[23] P. J. Steinhardt, D. R. Nelson, and M. Ronchetti, Phys. Rev. B **28**, 784 (1983).
[24] J. D. Honeycutt and H. C. Andersen, J. Chem. Phys. **91**, 4950 (1987).
[25] A. S. Clarke and H. Jónsson, Phys. Rev. E **47**, 3975 (1993).
[26] N. Jakse and A. Pasturel, J. Chem. Phys. **120**, 6124 (2004).
[27] F. H. M. Zetterling, M. Dzugutov, and S. I. Simdyankin, J. Non-Cryst. Solids **293-295**, 39 (2001).
[28] S. Valkealahti and M. Manninen, J. Phys.: Condens. Matter **9**, 4041 (1997).